

Detection of spin current through a quantum dot with Majorana bound states

Ning Wang(王宁), Xingtao An(安兴涛), and Shuhui Lv(吕树慧)

Citation: Chin. Phys. B, 2021, 30 (**10**): 100302. DOI: 10.1088/1674-1056/abff1c
Journal homepage: http://cpb.iphy.ac.cn; http://iopscience.iop.org/cpb

What follows is a list of articles you may be interested in

Detection of spin current through a quantum dot with Majorana bound states

Ning Wang(王宁), Xingtao An(安兴涛), and Shuhui Lv(吕树慧)
Chin. Phys. B, 2021, 30 (**10**): 100302. DOI: 10.1088/1674-1056/abff1c

Influences of spin-orbit interaction on quantum speed limit and entanglement of spin qubits in coupled quantum dots

M Bagheri Harouni
Chin. Phys. B, 2021, 30 (**9**): 090301. DOI: 10.1088/1674-1056/abeef4

Electron transfer properties of double quantum dot system in a fluctuating environment

Lujing Jiang(姜露静), Kang Lan(蓝康), Zhenyu Lin(林振宇), and Yanhui Zhang(张延惠)
Chin. Phys. B, 2021, 30 (**4**): 040307. DOI: 10.1088/1674-1056/abd759

Geometric phase of an open double-quantum-dot system detected by a quantum point contact

Qian Du(杜倩), Kang Lan(蓝康), Yan-Hui Zhang(张延惠), Lu-Jing Jiang(姜露静)
Chin. Phys. B, 2020, 29 (**3**): 030302. DOI: 10.1088/1674-1056/ab6963

Plasmon mediated entanglement dynamics of distant quantum dots

Misbah Qurban, Rabia Tahira, Guo-Qin Ge(葛国勤), Manzoor Ikram
Chin. Phys. B, 2019, 28 (**3**): 030304. DOI: 10.1088/1674-1056/28/3/030304

Detection of spin current through a quantum dot with Majorana bound states*

Ning Wang(王宁), Xingtao An(安兴涛), and Shuhui Lv(吕树慧)†

School of Sciences, Hebei University of Science and Technology, Shijiazhuang 050018, *China*

(Received 23 December 2020; revised manuscript received 19 April 2021; accepted manuscript online 8 May 2021)

The spin transport properties are theoretically investigated when a quantum dot (QD) is side-coupled to Majorana bound states (MBSs) driven by a symmetric dipolar spin battery. It is found that MBSs have a great effect on spin transport properties. The peak-to-valley ratio of the spin current decreases as the coupling strength between the MBS and the QD increases. Moreover, a non-zero charge current with two resonance peaks appears in the system. In the extreme case where the dot–MBS coupling strength is strong enough, the spin current and the charge current are both constants in the non-resonance peak range. When considering the effect of the Zeeman energy, it is interesting that the resonance peak at the higher energy appears one shoulder. And the shoulder turns into a peak when the Zeeman energy is big enough. In addition, the coupling strength between the two MBSs weakens their effects on the currents of the system. These results are helpful for understanding the MBSs signature in the transport spectra.

Keywords: Majorana bound states, quantum dot, spin current, Green's function

PACS: 03.67.Lx, 73.63.Kv, 73.23.–b, 74.78.Na **DOI:** 10.1088/1674-1056/abff1c

1. Introduction

Majorana fermions (MFs) are a special type of particles which are their own antiparticles and obey non-Abelian statistics.[1] They have attracted a great deal of attention due to their fundamental importance and potential applications in the quantum computation.[2,3] In contrast to ordinary quantum computations, quantum computations using MFs do not require quantum error correction since a widely separated pair of MF bound states are immune to local sources of decoherence due to their nonlocal topological nature.[4]

Initially, Majorana bound states (MBSs) can be realized at the ends of one-dimensional quantum wire by inducing superconductivity on semiconductor wire with strong spin–orbit coupling and subject to an external magnetic field.[5–7] So far, many different schemes to create MBSs have been proposed and implemented, such as magnetic atoms on the surface of superconductors[8,9] and topological Josephson junctions.[10–12] But most experimental reports about the existence of MBSs focus on the nanowire setup.[13–16] Several suggestions have been made to detect and verify the existence of MBSs by different transport signatures. The differential conductance at zero bias voltage is e^2/h when tunneling into a quantum dot (QD) side-coupled to MBSs.[17,18] Other suggestions include 4π periodic Majorana–Josephson currents[19,20] and Majorana–Josephson interferometer.[21] Recently, some works mainly focus on the signatures associated with spin in electrical transport through a Majorana nanowire.[22,23]

In this paper, we investigate the spin and the charge currents of the system when the QD is side-coupled to MBSs driven by a symmetric dipolar spin battery. We find that MBSs have a great effect on spin transport properties. With the increase of the coupling strength between the MBS and the QD, the peak-to-valley ratio of the spin current decreases. And a non-zero charge current with two resonance peaks appears in the system. Furthermore, the coupling strength between the two MBSs weakens their effects on the currents of the system.

This paper is organized as follows. In Section 2, we present the Hamiltonian of our system and detail the algebraic expressions of the current obtained by the nonequilibrium Green's function. The numerical results and analysis are given in Section 3. Finally, conclusions are drawn in Section 4.

2. Model and formula

In this section, we first present the setup of our system, as shown in Fig. 1. In Fig. 1(a), a QD is side-coupled to a topological wire hosing two MBSs driven by a symmetric dipolar spin battery. The MBSs emerge at two ends of the nanowire which is engineered by applying a strong magnetic field along its axis in proximity to an s-wave superconductor. Due to the proximity effect of the s-wave superconductor, the nontrivial superconductor phase resembles the p + ip superconductor phase that has two separated MBSs at two ends of the nanowire. In Fig. 1(b), a QD is side-coupled to normal spin-polarized fermions.

*Project supported by Natural Science Fund for Colleges and Universities in Hebei Province, China (Grant No. ZD2017031) and the Doctoral Initial Funding of Hebei University of Science and Technology (Grant No. 1181291).

†Corresponding author. E-mail: vshuhui@hebust.edu.cn

© 2021 Chinese Physical Society and IOP Publishing Ltd

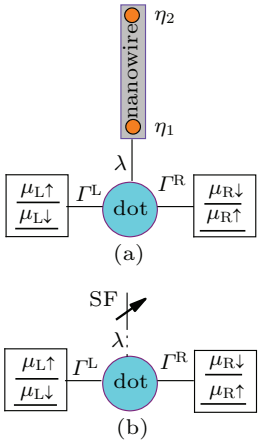


Fig. 1. Illustration of the proposed structure. (a) A QD coupled to a symmetric dipolar spin battery and side-coupled to a topological superconductor wire hosing two MBSs, η_1 and η_2. (b) A QD coupled to a symmetric dipolar spin battery and side-coupled to normal spin-polarized fermions.

In our considered system, the electron motion can be well described by[24,25]

$$H = H_{\text{leads}} + H_{\text{dot}} + H_{\text{d}-\alpha} + \text{i}\varepsilon_{\text{M}}\eta_1\eta_2 + \lambda(d_\downarrow - d_\downarrow^\dagger)\eta_1, \quad (1)$$

where $H_{\text{leads}} = \sum_{k\sigma}\sum_{\alpha=\text{L,R}}\varepsilon_{k\sigma}c_{k\sigma\alpha}^\dagger c_{k\sigma\alpha}$ describes the conduction electrons in the left (L) and right (R) leads and $c_{k\sigma\alpha}^\dagger$ ($c_{k\sigma\alpha}$) denotes the creation (annihilation) operator for electrons with momentum k and spin $\sigma \in (\uparrow\downarrow)$ in the lead α. $H_{\text{dot}} = \sum_\sigma \varepsilon_\sigma d_\sigma^\dagger d_\sigma + U d_\uparrow^\dagger d_\uparrow d_\downarrow^\dagger d_\downarrow$ is the Hamiltonian for the interacting single-level QD, where $\varepsilon_\sigma = \varepsilon_{\text{d}} + \sigma V_{\text{Z}}/2$ is the single energy level of the QD and U is the intradot Coulomb interaction energy, V_{Z} is the Zeeman energy, and $d_\sigma^\dagger$ (d_σ) denotes the creation (annihilation) operator for electrons with spin-σ in QD. $H_{\text{d}-\alpha} = \sum_{k\sigma}\sum_{\alpha=\text{L,R}} V_{k\alpha}(c_{k\alpha\sigma}^\dagger d_\sigma + \text{H.c.})$ describes the coupling between the QD and the leads.

The fourth term of H characterizes the coupling between the MFs η_1 ($=\eta_1^\dagger$) and η_2 ($=\eta_2^\dagger$) in the MBSs where the overlap amplitude ε_{M} depends on the wire parameters, $\varepsilon_{\text{M}} \sim \text{e}^{-l/\xi}$. l is the length of the wire and ξ is the superconducting coherence length. The last term of H describes the coupling between the QD and MBS, and λ is the coupling strength.

It is useful to change the Majorana fermion representation to an ordinary fermion representation by defining $\eta_1 = \frac{1}{\sqrt{2}}(f^\dagger + f)$ and $\eta_2 = \frac{\text{i}}{\sqrt{2}}(f^\dagger - f)$, where $f^\dagger$ (f) creates (annihilates) a fermion and $f^\dagger f = \{0,1\}$ counts the occupation of the corresponding states. The last two terms in H become

$$H_{\text{MBS}} = \varepsilon_{\text{M}}(f^\dagger f - 1/2) + \frac{1}{\sqrt{2}}\lambda(d_\downarrow - d_\downarrow^\dagger)(f + f^\dagger). \quad (2)$$

In this paper, considering separately the chemical potentials of the leads to be $\mu_{\text{L}\sigma} = \sigma\frac{V_{\text{s}}}{2}$ and $\mu_{\text{R}\sigma} = \overline{\sigma}\frac{V_{\text{s}}}{2}$, we pay attention to the electron properties of the system driven by the symmetric dipolar spin battery. Here, V_{s} is the magnitude of spin bias. By means of the Keldysh nonequilibrium Green's functions formalism, the electron current J_σ for spin component σ can be calculated by the following standard formula:

$$J_\sigma = \frac{\text{i}e}{h}\int\frac{\text{d}\varepsilon}{2\pi}[f_{\text{L}\sigma}(\varepsilon) - f_{\text{R}\sigma}(\varepsilon)]T_\sigma(\varepsilon), \quad (3)$$

where $f_{\alpha\sigma} = 1/\{\exp[(\varepsilon - \mu_{\alpha\sigma})/k_{\text{B}}T] + 1\}$ is the Fermi distribution function of spin-σ electron in lead-α and $\mu_{\alpha\sigma}$ is the chemical potential. The spin and charge currents are defined as $J_{\text{s}} = h(J_\uparrow - J_\downarrow)/2$ and $J_{\text{e}} = e(J_\uparrow + J_\downarrow)/2$, respectively. $T_\sigma(\varepsilon)$ is the transmission coefficient for spin σ electrons, and can be written as

$$T_\sigma(\varepsilon) = \text{Tr}\frac{\Gamma^{\text{L}}\Gamma^{\text{R}}}{\Gamma^{\text{L}} + \Gamma^{\text{R}}}[G^{\text{r}}(\varepsilon) - G^{\text{a}}(\varepsilon)], \quad (4)$$

where $\Gamma^\alpha = 2\pi\sum_k V_{\alpha k}^* V_{\alpha k}\delta(\varepsilon - \varepsilon_{\alpha k\sigma})$ is the line-width function or coupling strength between the QD and the leads. $G^{\text{r}}(\varepsilon)$ ($G^{\text{a}}(\varepsilon)$) is the standard retarded (advanced) Green's function of the QD and MBS in the presence of the coupling to the leads. The standard equation of motion method yields an exact expression for the Green's function[17,26]

$$G_\sigma^{\text{r}}(\varepsilon) = \frac{1 + U\widetilde{K}(1 - \lambda^4 k_1 k_2)}{[\varepsilon - \varepsilon_\sigma - \lambda^2 k(1 + \lambda^2 k_2)] - \Sigma_\sigma^{\text{r}}[1 + U\widetilde{K}(1 - \lambda^4 k_1 k_2)]}, \quad (5)$$

where $k = \varepsilon/(\varepsilon^2 - \varepsilon_{\text{M}}^2)$, $k_1 = k/(\varepsilon + \varepsilon_\sigma + U - \lambda^2 k_2)$, $k_2 = k/(\varepsilon + \varepsilon_\sigma - \lambda^2 k)$ and $\widetilde{K} = n_{\overline{\sigma}}/(\varepsilon - \varepsilon_\sigma - U - \lambda^2 k(1 + \lambda^2 k_1))$. $\Sigma_\sigma^{\text{r}} = -\text{i}/2(\Gamma^{\text{L}} + \Gamma^{\text{R}})$ is the retarded self-energy, and $n_{\overline{\sigma}}$ is the intradot electron occupation number at the spin state $\overline{\sigma}$. In the corresponding calculations, $\overline{\sigma}$ stands for '–' while σ stands for '+'. n_σ needs to be calculated self consistently and its self-consistent equation is

$$n_\sigma = \int_{-\infty}^{+\infty}\frac{\text{d}\varepsilon}{2\pi}\text{Im}G_\sigma^<(\varepsilon). \quad (6)$$

The correlation Green's function $G^<(\varepsilon)$ can be calculated from the Keldysh equation, $G^<(\varepsilon) = G^{\text{r}}(\varepsilon)\Sigma^<(\varepsilon)G^{\text{a}}(\varepsilon)$, where the lesser self-energy $\Sigma^<(\varepsilon)$ is related to the retarded and the advanced self-energies through $\Sigma^<(\varepsilon) = -\Sigma_\alpha[\Sigma_\alpha^{\text{r}}(\varepsilon) - \Sigma_\alpha^{\text{a}}(\varepsilon)]f_{\alpha\sigma}(\varepsilon)$.

3. Numerical results and discussion

In the numerical investigation, we consider the case of symmetric barriers with $\Gamma^{\text{L}} = \Gamma^{\text{R}} = \Gamma/2$, $V_{\text{s}} = 0.5$, $U = 12$, and choose the line-width function Γ as the energy unit. Figure 2 shows the spin current J_{s}, the charge current J_{e} and the spin-polarized current J_σ as a function of the dot level ε_{d} with various dot–MBS coupling λ for $\varepsilon_{\text{M}} = 0$ and $V_{\text{Z}} = 0$.

As we know, in the absence of the topological superconductor wire and MBSs (i.e., $\lambda = 0$), the spin current has two sharp resonance peaks at $\varepsilon_{\text{d}} = 0$ and $\varepsilon_{\text{d}} = -U$, which are two possible conducting channels for tunneling through the QD, as

shown by the black solid line in Fig. 2(a). The energy separation between the two peaks is just the Coulomb interaction energy of the QD. The spin polarization current is with the opposite direction and the same amplitude, resulting in zero charge current, as shown by the black solid line in Fig. 2(b). When the QD is side-coupled to the MBS (i.e., $\lambda \neq 0$), the spin current in the non-resonance peak range increases as λ increases. Although the magnitudes of the spin current at resonance peaks are suppressed, they remain constant with λ increasing, as shown in Fig. 2(a). The reason is that only the spin-down electrons are coupled to the MBS. The peak-to-valley ratio of the spin-down current $J_\downarrow$ decreases as λ increases, but the spin-up current $J_\uparrow$ is weakly dependent on λ, as shown in Figs. 2(c) and 2(d). According to the expressions of the spin current and the charge current, it can be found that the effect of the MBS on the spin current is mainly in the non-resonance range. Moreover, a non-zero charge current with two resonance peaks appears in the system, and it also increases as λ increases.

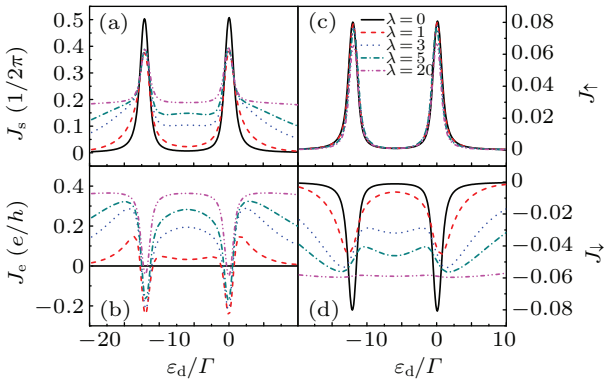


Fig. 2. The spin current J_s (a), the charge current J_e (b), the spin-polarized currents $J_\uparrow$ (c) and $J_\downarrow$ (d) as a function of the QD level ε_d with different dot–MBS coupling strength, $\varepsilon_M = 0$ and $V_Z = 0$.

Furthermore, we compute the limiting case, $\lambda = 20$. As shown in Figs. 2(c) and 2(d), $J_\uparrow$ is only slightly suppressed, but $J_\downarrow$ remains almost constant. As a result, the spin current and the charge current in non-resonance peak range are constants, as shown in Figs. 2(a) and 2(b).

In order to clarify the genuine effect of the MBS, we calculate the current when the QD is coupled to normal spin-polarized fermions. Figure 3 shows the spin and the charge currents as a function of the QD energy when the QD is coupled to normal spin polarization fermions under the same configuration. The coupling energy for spin polarization and the Zeeman energy for the QD are both set to zero with $\varepsilon_M = 0$ and $V_Z = 0$.

In Fig. 3(a), we can find the resonance peaks of the spin current are suppressed, but they remain at the same position, when the QD is coupled to normal spin polarization fermions. With the increase of λ, the spin current is weakly dependent on it. For the charge current, it is strictly zero when $\lambda = 0$; while $\lambda \neq 0$, there are two negative peaks at $\varepsilon_d = 0$ and $\varepsilon_d = -U$, as shown in Fig. 3(b). It means that the spin-up electrons are more likely to be localized in the QD.

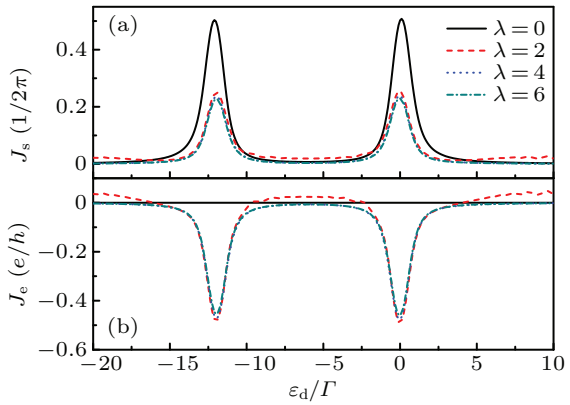


Fig. 3. The spin current J_s (a) and the charge current J_e (b) as a function of the QD level ε_d with different dot–MBS coupling strength when the QD is coupled to normal spin polarization fermions with $\varepsilon_M = 0$ and $V_Z = 0$.

It is well-known that there are three necessary conditions for the induction of MFs at both ends of nanowire: strong Rashba spin–orbit coupling, proximity-induced s-wave superconductivity and magnetic field. Because the QD and nanowire can be different materials and have different g factors, the Zeeman splitting energy induced by magnetic field in nanowire is different from that in the QD. Next, we study the effect of the Zeeman splitting energy in the QD on the system.

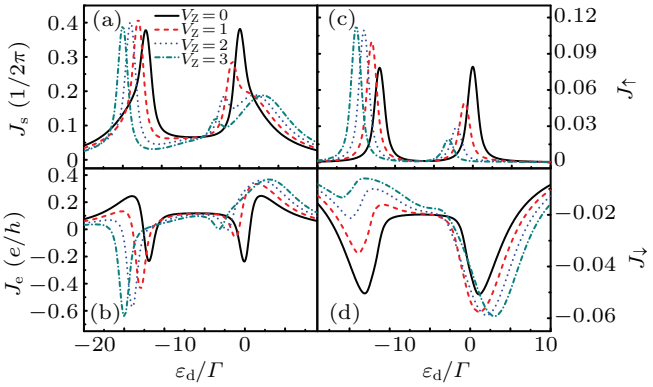


Fig. 4. The spin current J_s (a), the charge current J_e (b), the spin-polarized currents $J_\uparrow$ (c) and $J_\downarrow$ (d) as a function of the QD level ε_d with different Zeeman energy V_Z when the QD is coupled to MBS, $\lambda = 2$.

In Fig. 4, we plot the spin current, the charge current and the spin polarized currents as a function of the QD level ε_d for $\lambda = 2$, with different values of V_Z, when the QD is coupled to the MBS. As V_Z increases, the two resonance peaks move towards the lower energy, and the distance between the two resonance peaks remains constant. Meanwhile, the resonance peak at the higher energy is suppressed. The characters are similar to the case of the QD coupled to normal polarization fermions, as shown in Fig. 5. When the QD is coupled to the MBS, it is interesting that the resonance peak at the higher energy appears one shoulder at $\varepsilon_d \approx V_Z$. When V_Z is larger than λ, the shoulder changes into a peak at $\varepsilon_d \approx V_Z$. The reason is

that the resonance peak of the spin-polarized current $J_\downarrow$ moves towards the higher energy and its range widens as the Zeeman energy V_Z increases, as shown in Fig. 4(d).

We also calculate the spin current and the charge current under different Zeeman energy for the QD coupled to normal polarization fermions, as shown in Fig. 5. Different from the case of the QD coupled to the MBS, both the spin current and the charge current move towards the lower energy as the Zeeman energy V_Z increases, and the distance between the two resonance peaks remains constant. However, with the increase of Zeeman energy, the amplitude of the resonance peak at the higher energy is suppressed, and that at the lower energy is increasing. Furthermore, the charge current is always negative. That is also different from the case of the QD coupled to the MBS in which the charge current can be positive or negative.

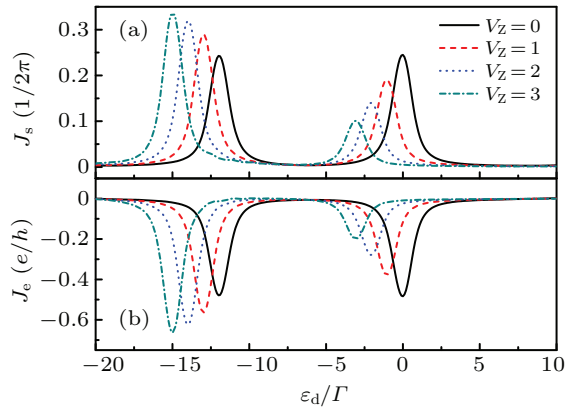


Fig. 5. The spin current J_s (a) and the charge current J_e (b) as a function of the QD level ε_d with different Zeeman energy V_Z when the QD is coupled to normal spin polarization fermions, $\lambda = 2$.

In practice, the length of the nanowire cannot be so long that there is no interaction between the MBSs at both ends of the nanowire, so we calculate the effect of the coupling strength between the two MBSs on the electrical current. Figure 6 shows the spin current and the charge current as a function of the QD energy with different MBS–MBS coupling strength ε_M.

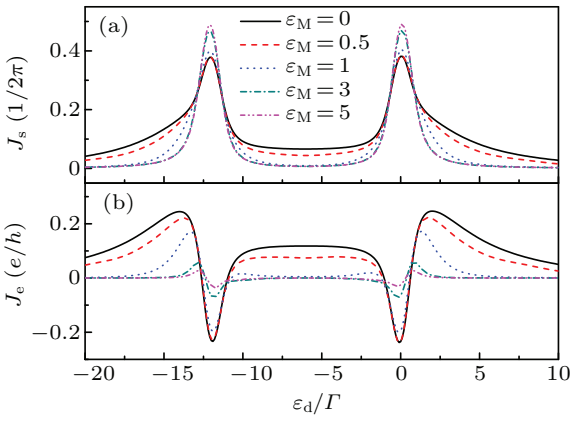


Fig. 6. The spin current J_s (a) and the charge current J_e (b) as a function of the QD level ε_d with different ε_M when the QD is coupled to the MBS. The other parameters are $V_Z = 0$, $\lambda = 2$.

As shown in Fig. 6, the magnitude of the two resonance peaks of the spin current increases with ε_M increasing. Their positions remain the same, and their widths become narrower. The absolute value of the charge current decreases with ε_M increasing, and the charge current may decrease to absolute zero when it is large enough. Comparing Figs. 2 and 6, it can be found that the spin current and the charge current return to the case of $\lambda = 0$ in Fig. 2 with ε_M increasing. That is to say the interaction between MBSs cancels out the interaction between the QD and the MBS. Therefore, in order to enhance the effect of the MBS on the system, ε_M should be small enough.

4. Conclusion

In this paper, we have studied the spin transport properties of the QD side-coupled to MBSs driven by a symmetric dipolar spin battery. The MBSs can be emerged at two ends of one-dimensional quantum wire which is in proximity to an *s*-wave superconductor with strong spin–orbit coupling and subjected to an external magnetic field. Since the MBSs only interact with the spin-down electrons in the QD, the spin-up polarization current is weakly dependent on the coupling strength between the QD and the MBS, and the peak-to-vally ratio of the spin-down polarization current decreases as the coupling strength increases. This causes the spin current to increase as the coupling strength between the QD and the MBS rises, except for the positions at the two resonance peaks. So is the charge current. Furthermore, it is found that the coupling strength between the two MBSs weakens their effects on the system.

References

[1] Alicea J, Oreg Y, Refael G, von Oppen F and Fisher M P A 2011 *Nat. Phys.* **7** 412
[2] Wilczek F 2009 *Nat. Phys.* **5** 614
[3] Das A, Ronen Y, Most Y, Oreg Y, Heiblum M and Shtrikman H 2012 *Nat. Phys.* **8** 887
[4] Nayak C, Simon S H, Stern A, Freedman M and Das Sarma S 2008 *Rev. Mod. Phys.* **80** 1083
[5] Aguado R 2017 *Nuovo Cimento* **40** 523
[6] Sau J D, Lutchyn R M, Tewari S and Das Sarma S 2010 *Phys. Rev. Lett.* **104** 040502
[7] Sato M, Takahashi Y and Fujimoto S 2010 *Phys. Rev. B* **82** 134521
[8] Nadj-Perge S, Drozdov I K, Li J, Chen H, Jeon S, Seo J, MacDonald A H, Bernevig B A and Yazdani A 2014 *Science* **346** 602
[9] Ruby M, Heinrich B W, Peng Y, von Oppen F and Franke K J 2017 *Nano Lett.* **17** 4473
[10] Park S and Recher P 2015 *Phys. Rev. Lett.* **115** 246403
[11] Scharf B, Pientka F, Ren H, Yacoby A and Hankiewicz E M 2019 *Phys. Rev. B* **99** 214503
[12] Pang Y, Wang J H, Lyu Z Z, Yang G, Fan J, Liu G T, Ji Z Q, Jing Z N, Yang C L and Lu L 2016 *Chin. Phys. B* **25** 117402
[13] Nichele F, Drachmann A C C, Whiticar A M, O'Farrell E C T, Suominen H J, Fornieri A, Wang T, Gardner G C, Thomas C, Hatke A T, Krogstrup P, Manfra M J, Flensberg K and Marcus C M 2017 *Phys. Rev. Lett.* **119** 136803

[14] Zhang H, Liu C X, Gazibegovic S, Xu D, Logan J A, Wang G, van Loo N, Bommer J D S, de Moor M W A, Car D, het Veld R L M O, van Veldhoven P J, Koelling S, Verheijen M A, Pendharkar M, Pennachio D J, Shojaei B, Lee J S, Palmstrøm C J, Bakkers E P A Sarma M S D and Kouwenhoven L P 2018 *Nature* **556** 74
[15] Laroche D, Bouman D, van Woerkom D J, Proutski A, Murthy C, Pikulin D I, Nayak C, van Gulik R J J, Nygård J, Krogstrup P, Kouwenhoven L P and Geresdi A 2019 *Nat. Commun.* **10** 245
[16] Liu J, Li K M, Chi F, Fu Z G and Zhang P 2020 *Chin. Phys. B* **29** 077302
[17] Liu D E and Baranger H U 2011 *Phys. Rev. B* **84** 201308
[18] Wang N, Lv S H and Li Y X 2014 *J. Appl. Phys.* **115** 083706
[19] Sticlet D, Sau J D and Akhmerov A 2018 *Phys. Rev. B* **98** 125124
[20] Frombach D and Recher P 2020 *Phys. Rev. B* **101** 115304
[21] Li C A, Li J and Shen S Q 2019 *Phys. Rev. B* **99** 100504
[22] Yang F B 2019 *Phys. E* **109** 164
[23] Schuray A, Rammler M and Recher P 2020 *Phys. Rev. B* **102** 045303
[24] Weymann I and Wójcik K P 2017 *Phys. Rev. B* **95** 155427
[25] Lee M, Lim J S and López R 2013 *Phys. Rev. B* **87** 241402
[26] Leijnse M and Flensberg K 2011 *Phys. Rev. B* **84** 140501